The Liverpool Telescope: performance and first results

I. A. Steele[a], R. J. Smith[a], P. C. Rees[b], I. P. Baker[b] S. D. Bates[a] M. F. Bode[a], M. K. Bowman[b], D. Carter[a], J. Etherton[a], M. J. Ford[b], S. N. Fraser[a], A. Gomboc[a], R. D. J. Lett[b], A. G. Mansfield[b], J. M. Marchant[a], G. A. Medrano-Cerda[b], C. J. Mottram[a], D. Raback[a], A. B. Scott[a], M. D. Tomlinson[a] and R. Zamanov[a]

[a]Astrophysics Research Instititue, Liverpool JMU, Birkenhead CH41 1LD, UK
[b]Telescope Technologies Ltd, Morpeth Wharf, Birkenhead, CH41 1NQ, UK

ABSTRACT

The Liverpool Telescope is a 2.0 metre robotic telescope that is operating unattended at the Observatorio del Roque de Los Muchachos, Spain. This paper gives an overview of the design and implementation of the telescope and its instrumentation and presents a snapshot of the current performance during the commissioning process. Science observations are under way, and we give brief highlights from a number of programmes that have been enabled by the robotic nature of the telescope.

Keywords: telescopes, robotic, automated, design, performance, science

1. INTRODUCTION

The Liverpool Telescope[1] is a 2.0 metre fully robotic telescope at the Roque de Los Muchachos Observatory, La Palma, Spain. Its primary science drivers are enable monitoring observations of variable sources on timescales of minutes – years as well as providing fast response to targets of opportunity. In addition a small fraction of the time is set aside for schools[2] and public understanding of science.

The telescope achieved first light in July 2003, and is presently undergoing commissioning in parallel with carrying out the initial science programme. This paper aims to give a basic overview of the telescope, describe the current and planned performance of the telescope, and briefly outline some of the early science observations that have been carried out. We have attempted to keep details to a minimum in this publication as in many cases more information is available in other publications. We have however tried to collate as many of the relevant references as possible in order that the interested reader may "home in" on those areas which are of interest.

2. SYSTEM DESCRIPTION

The Liverpool Telescope was designed and built by Telescope Technologies Limited (a subsidiary company of Liverpool JMU) with robotic control software and instrumentation developed by the Astrophysics Research Institute of JMU. It is of altitude-azimuth design with a mechanical Cassegrain derotator. Provision in the design is also made for two Nasmyth foci with mechanical derotation, although these are not presently fitted.

In Table 1 we list the key performance specifications for the Liverpool Telescope. These were derived at the start of the project from an analysis of the science use cases, and served to constrain the design and implementation of all telescope and instrument systems.

2.1. Optical Design

The optical design of the telescope primary and secondary mirrors is Ritchey-Chretien Cassegrain. The primary mirror has clear aperture 2000 mm and a central bore of 450 mm. The edge thickness of the primary is 200 mm and it has a machined flat back. Its focal ratio is f/3, corresponding to a radius of curvature of -12000 mm with a conic constant of -1.0703. The primary mirror is manufactured from Astrosital (thermal expansion coefficient $0.0 \times 10^{-7} \pm 0.6 \times 10^{-7}$) and has invar pads bonded to the outer edge of the mirror for attaching both the lateral support and radial defining systems.

The secondary mirror has a clear aperture of 617 mm and a centre thickness of 110 mm. It has a radius of curvature of -4813 mm with a conic constant of -4.179 and is manufactured from Schott Glass Zerodur. Invar

Table 1. Liverpool Telescope Key Performance Specifications

Item	Specification
Clear Aperture	2.0 metres
Focal Length	20.0 metres
Image quality (on axis)	< 0.4 arcsec (80% encircled energey)
Image quality (6 arcmin radius)	< 0.6 arcsec (80% encicrled energy)
Field flatness	$< \pm 50\mu$m within 6 arcmin radius
Pointing Accuracy (alt = 20–88 °)	< 2 arcsec rms
Open Loop Tracking Accuracy	< 0.4 arcsec in 10 minutes
Short Period Tracking Accuracy	< 0.2 arcsec over all timescales < 1 minute
Closed Loop Tracking Accuracy	< 0.2 arcsec in one hour
Slew Speed (all axes)	2°/second
Acceleration (all axes)	0.3°/second/second
Focus Tracking	$< 10\mu$m secondary movement

pads are bonded to the flat back for attaching the secondary mirror mechanism in a whiffle tree arrangement, while the lateral support pad is bonded to the mirror inside a rear bore.

The primary to secondary distance is designed to be 4315.385 mm, with a secondary to focal plane distance of 5615.385 mm. The system focal ratio is f/10, giving an image scale of 97 μm/ arc second.

Baffles are mounted on the structure to control stray light and also to protect the optics and their support. An upper baffle surrounds the secondary mirror, a main Cassegrain baffle is mounted from the telescope centre section, and a further baffle surrounds the primary mirror between the mirror cell and the telescope centre section. This latter baffle incorporates the 2.0 m aperture ring (aperture stop) and serves to minimize wind-shake on the primary as well as to restrict stray light.The obscuration of the beam due to the secondary assembly and its support vanes totals 18.5%.

A Cassegrain Acquisition and Guidance (A&G) unit provides a retractable, tertiary fold mirror that can be rotated about the optical axis to direct light into one of four side ports, or removed from the beam to allow the beam to pass to a straight-through port. The unvignetted field of view is 42 arc minutes at the straight through port and 7.5 arc minutes at the folded side ports. Provision has been made in the design of the A&G unit for a two-element wide-field corrector, fabricated from fused silica, that would provide a high degree of field curvature correction for imaging applications if it were needed in future.

In this design, focus adjustment is provided by the axial motion of the secondary mirror. The pole of the secondary is mechanically aligned with the Cassegrain rotator axis to within ± 100 μm. No actuation or adjustment of the secondary mirror is provided for optical alignment: fine optical alignment during operation being provided by actuators incorporated in the primary mirror support. This approach is intended to simplify the telescope design and optimize the maintainability of the system.

2.2. Structure

A key design objective of this telescope is its accurate astronomical operation outside of conventional dome enclosure (Section 2.5). As a result, particular emphasis has been placed throughout the design programme[3,4] to maintain high levels of structural stiffness and correspondingly high structural natural frequencies. The first mode of structural oscillation has been designed to be above 15 Hz, allowing the control system to control the effects of wind buffeting on the telescope tracking performance.

The telescope tube carries the supports for the primary and secondary mirrors. It is of conventional Serrurier truss design, the truss having been optimized for high stiffness and low differential displacement between primary and secondary sections. Mechanically, the optical axis is defined by the centre of rotation of the Cassegrain rotator bearing and the pole of the secondary mirror: the pole of the primary mirror being brought into coincidence with this axis during optical alignment. This optical axis is arranged to intersect, and be orthogonal to, the altitude axis: defined by the centre of rotation of the altitude trunnion bearings.

The telescope tube assembly rests upon an azimuth gimbal whose centre of rotation provides the datum for the alignment of the entire telescope. The azimuth and altitude axes are each supported by hydrostatic bearings (Section 2.3.3), using a thermally controlled hydraulic oil supply. The altitude bearing comprises four load-bearing shoes and two guide bearings, providing a lateral preload. The azimuth bearing comprises three load bearing shoes and three adjacent guide bearings, providing a lateral preload.

Derotation bearings at each focal station are realized using crossed roller bearings, with the option of optical derotation at Nasmyth focal stations. The limits of the range of motion of each telescope axis are azimuth -180° – +360°, altitude 20° – 90°, and Cassegrain ±240°.

2.2.1. Primary Mirror Support

The primary mirror support system comprises both the axial and lateral support (and defining) systems for the primary mirror. The axial support units are single acting pneumatic actuators. The actuators are divided into three sectors to provide a kinematic support of the mirror. The actuator design employs a diaphragm seal to apply force demands from the primary mirror control system to the mirror. The force in each actuator varies with the elevation angle of the telescope tube. Three axial defining units define the axial position of the primary mirror, one for each of the axial support sectors. Each defining unit includes a load cell (which provides force feedback for the primary mirror control system).

The lateral support units are double acting pneumatic actuators. Again diaphragm seals apply force demands from the primary mirror control system to the mirror. One of the actuating chambers is in opposition to the force chamber to provide a pre-load force in the actuator. Three radial defining units define the lateral position of the mirror with a load cell which provides force feedback for the control system.

2.2.2. Auxiliary Mechanisms

Auxiliary mechanisms such as secondary focus drive, the folding mirror and primary mirror fine alignment are realized as precision stepper motor actuated systems. Key to the optical performance of the telescope is the secondary mirror assembly and its actuation. The secondary mirror cell provides a mechanical axial and lateral support, and is mounted to a counterbalanced focus drive to minimize out-of-balance torques on the telescope tube.

2.3. Control

2.3.1. Control Philosophy

The axes motion control system for the Liverpool 2.0 m Telescope applies to the following axes:

- Azimuth axis
- Altitude axis
- Cassegrain rotator

In addition to the these telescope axes of motion, a further real-time control system is used for the pneumatic support of the primary mirror.

For each axis, the design of the axis motion control is based primarily upon the exploitation of commercial off-the-shelf electrical, electronic and electro-mechanical components as much as is practicable. Emphasis has also been placed upon low servicing overheads.

The key architectural features of the axes motion control system for the Liverpool Telescope are as follows:

- An in-house controller, generic to all telescope axes.
- A distributed architecture.

- Intel-based embedded industrial microcomputers running the QNX real-time operating system.
- A 10/100 baseT network architecture (CAT 5 compliant hardware), running Internet protocols over a switched Ethernet local area network.
- Timing signals distributed for the real-time components of the system using IRIG-B originating from a GPS receiver.

An in-house controller was chosen in preference to a "black-box" solution for the following reasons:

1. because it offered greater flexibility for I/O within the system;
2. because it facilitated the development of more specialist controller algorithms than those commercially available;
3. because it enabled the use of a standard computing platform that could be modularised and developed for different axis applications;
4. because the telescope product life-cycle would be less affected by controller obsolescence (if individual components of an in-house system become obsolete it is more likely that they can be replaced without major system design changes).

A distributed control architecture, applying to axis control, auxiliary and services systems, was chosen so that the architecture could accommodate control and telemetry throughout a whole observatory in an integrated way. A distributed architecture also facilitates the development and inclusion of modular hardware targeted at discrete sub-systems, which again reduces operational costs due to improved spares redundancy. Distributed systems are readily scaleable, reduce cabling infrastructure, and facilitate addition of further axes configurations or auxiliary sub-systems. The modularity gain of these systems also increased testability, both during development and in operation. The choice of real-time operating system was influenced by the need for a genuine real-time, micro-kernel operating system. The features offered by the QNX operating system are that it is designed specifically for distributed operation, it is scaleable, cost-effective, can be used in highly embedded systems and is POSIX compliant. The fault tolerance of the operating system is demonstrated by its use in safety-critical applications, including the Canadian nuclear industry.

2.3.2. Disturbance Rejection

A key factor in the performance of the axes control systems performance is their ability to compensate for the effects of external disturbances upon the system. The sources of such disturbances to each axis control system are as follows:

- Motion system friction
- Motor commutation ripple
- Motor cogging
- Out-of-balance moments
- Wind

The sources of friction include bearings, gearboxes, motors and ancillary assemblies (e.g. cable wraps).

Of particular importance is the effective rejection of disturbances due to the effects of wind upon the telescope. A principal design goal of the telescope is to operate outside of an enclosure in winds up to 80 km/hr and to operate to specification in this environment in winds significantly greater than 40 km/hr. The effective rejection of disturbances to the motion control system is dependent upon the bandwidth of the control system (i.e. the speed of response of the controller to a disturbance). The bandwidth is normally interpreted as the frequency at which there is a 3 dB reduction in the gain of control system with respect to zero frequency. In general, controller design for systems where systemic resonances exist in the same frequency range as external disturbances are difficult to implement and maintain. It is estimated from published data that the maximum frequency of significant wind disturbance is 10 Hz, assuming 80 km/hr winds. Hence the motor/gear box selection for each axis was based upon estimated resonances of 10 Hz. In addition, the natural frequency of the telescope structure was designed to be considerably above 10 Hz.

2.3.3. Bearing Choice

Hydrostatic bearings were chosen for the azimuth and altitude axes, because of the requirements for stiff, precise and extremely low friction bearings on these axes. For the azimuth axis, the hydrostatic bearing system is implemented using three master load-bearing pads and three radial guiding pads placed adjacent to the load-bearing pads. For the altitude axis, the hydrostatic bearing system is implemented using four master load-bearing pads (two either side of the centre section), with two axis defining pads placed one either side of the centre section. The entire hydrostatic bearing system is fed by a common oil supply and has a capacity of 50 l/min. A refrigeration unit keeps the oil close to the telescope ambient temperature. The Cassegrain rotator bearing is a slewing ring using crossed cylindrical roller bearings. A slewing ring was chosen because they can accommodate both radial and axial loads, as well as moment loads in any orientation. The compact design and large bore diameter allow the placement of drive equipment. The specific design of the slewing ring used at Cassegrain offers a stiff bearing arrangement capable of supporting the loads expected from the Cassegrain equipment.

2.3.4. Actuation Choice

Each telescope axis uses a multi-motor gear drive with an anti-backlash scheme. A 50% full load torque bias was adopted, based upon early control modelling results, although later testing has resulted in the use of lower percentages of the full load torques to improve control performance. The motor and gearbox selection was based primarily upon the estimated torques from wind, operational acceleration and friction. Because the application demands high accuracy and low speeds, the following choices were made for the motors:

- D.C. servo, operated in torque mode.
- Ironless rotor construction, chosen for zero cogging.
- High pole-count, yielding low commutation ripple.

The motors were sized for continuous rated torque and de-rated to allow for operation at altitude. Torque mode was chosen for the operation of the motors to facilitate greater flexibility for controller schemas, effective operation in anti-backlash mode, and to minimize the effects of digital/analogue converter resolution upon controller design. The gear box choice was based upon maximizing stiffness (with suitable mechanical interfacing), and not on the rated torque of the motor/gearbox combination. Consideration was also given to the compactness of design, the efficiency of the gear box, and the ability to back-drive (because of the requirements to operate in an anti-backlash configuration). Each motor is provided with a mounted brake and encoder. The brake is rated to several times the maximum system torque for safety. High resolution rotary encoders have been mounted co-axially with the motor rotor for the derivation of motor velocity feedback signals for the control system. Positional encoding used for control purposes (as opposed to safety interlocking purposes) is as follows:

- geared absolute rotary encoder;
- incremental tape encoder with reference mark coding using multiple read heads.

Here, the absolute encoder is used for system start-up (for determining the direction of travel for homing the incremental tape encoder) and for an intermittent health check on the encoder system during operation. The choice of incremental tape encoders for each of the axes has the following advantages:

- error reduction through averaging the encoder signals from two or more reading heads;

- the cancellation of slewing-ring run-out harmonics in the encoder data;
- The measurement and compensation of axis translation in the encoder data.

The encoding precision was calculated as a minimum of twenty times the accuracy of tracking required for each axis.

2.3.5. Timing Distribution

The motion control system requires both a high absolute accuracy time signal and a high accuracy synchronization signal. A high absolute accuracy time signal is implemented as a distributed time signal with an absolute accuracy of 50 ms, using a NTP Stratum 1 GPS-based server, supplying system time to network clients and the Telescope Control System for astrometric calculations via a Stratum 2 server. This signal is distributed via the local area network using Internet protocols. Synchronization and event time-stamping, required for the co-ordinated motion of high servo-rate axes control systems, is distributed using the IRIG-B protocol and provides an interrupt time pulse driven at 400 Hz with an absolute accuracy of 1 ms. For the control system for each axis, a minimum absolute accuracy of 125 ms is required for this distributed time signal.

2.3.6. Computing Systems

The computing system[5] may be divided into areas of different functionality, referred to here as "layers", because of their staged logical proximity to the telescope mechanisms. There are four distinct, integrated layers of software. These are the On-mount Layer, the Supervisory Layer, the Astrometric Layer and the Robotic Layer. These layers each comprise one or more applications and may run on single or distributed hardware as is appropriate.

The "On-mount Layer" is that closest to actual telescope hardware. It does not provide a direct user interface, but is controlled through the Supervisory Layer or by a higher level system via the Supervisory Layer.

The "Supervisory Layer" provides generic engineering control to the On-mount Layer, as well as various other off-mount hardware. It is also responsible for the supervisory control of the computing system, which means that it handles computer control authorization, state monitoring, and the orderly start-up and shutdown of the computing system as a whole. The Supervisory Layer is also responsible for monitoring and, subsequently, making available all status data. It provides the storage for this data as well as allowing it to be stored to any optional long-term media. This layer also provides storage of system-logs.

The Supervisory Layer software provides the central hub of communication to and from the low-level control software in the On-mount Layer. It maintains the engineering state model for the telescope and its control system. It is capable of detecting system failures and initiating recovery procedures. It is also capable of restarting software, as well as rebooting and/or power-cycling computer hardware via computer controlled power-switches. The Supervisory Layer provides a user interface for engineers to monitor and control the telescope at the machine level.

The "Astrometric Layer" provides co-ordinated high-level telescope control and astrometric transformations, within the context of astronomical observations. It is responsible for the astronomical calculations and provides the astrometric functions necessary for them. It converts demands in astronomical co-ordinate systems (e.g. Right Ascension and Declination) into sequenced engineering demands, which are sent via the Supervisory Layer software in order to control the telescope. The Astrometric Layer interacts with the user either directly with its own interactive interface, or via a network connection with the Robotic Layer.

The "Robotic Layer"[6] is a high level sequencing and scheduling system that interfaces both with the Astrometric Layer and the instrument control systems. An object-oriented database[7] is held locally at the telescope. This contains specifications of all observations that are to be carried out. A scheduling algorithm[8,9] is run on this database every time a new observation is to be executed. The chosen observation is then carried out by sequencing commands to the telescope and instruments.[10] Real time data pipelines running on all instruments feed back quality control data to the Robotic Layer to allow real-time evaluation of instrument and telescope performance, as well as the current observing conditions. This quality control data is used to both influence scheduling decisions and initiate attempted system recovery for malfunctioning systems.

The computing systems all reside on a local LAN, access to which is strictly controlled by firewalls.[11–13] Remote management is possible through a Virtual Private Network, with secure proxies to allow observers to interact with the observation database.

2.4. Instrumentation

All instruments interface to the LT using at the Acquisition & Guidance (A&G) Box. This has a rotating folding mirror that can direct the beam from the telescope to any one of four side ports, or can be retracted to allow the beam to pass straight through to a mounting plate at the bottom of the box. At both the side and straight through ports, the back focal distance is 75.0 mm, and instruments are designed to have their focus as close to this position as possible so that secondary focus movements are kept to a minimum when changing instruments. Overall up to five instruments can be mounted on the telescope at any time. The change time between instruments is < 40 seconds, and the fold mirror is specified to re-position itself repeatedly corresponding to a projected sky offset of < 0.15 arcsec. This allows targets acquired by one instrument to be placed accurately on the focal plane of another. As well as a stable mechanical interface to the telescope optical beam, the A&G box also provides access to electrical, network and fibre optic services to support the instrument. It also provides the mounting for the telescope autoguider.

The instrument suite[10] has been designed to address the basic imaging and spectroscopic needs of the majority of the science programme, which is mainly target of opportunity or monitoring observations of point sources (Section 4). Briefly they consist of:

- **RATCam** - a 2048x2048 pixel optical CCD imaging camera. This uses a closed cycle cooled E2V CCD42-40 detector giving a pixel scale of 0.135 arcseconds/pixel. Two, five position filter wheels hold Sloan $u'g'r'i'z'$ and Bessell BV filters. Readout and control of the filter wheels are both accomplished using SDSU Generation 2 controllers. This instrument is in regular use at the telescope, although some final tuning of the clock and bias voltages is still outstanding.
- **SupIRCam** - a 256x256 pixel near-IR imaging camera. This uses a closed cycle cooled Rockwell PICNIC array giving a pixel scale of 0.4 arcseconds/pixel. An internal cooled filter wheel provides JHK' filters. The instrument is currently mounted on the telescope without its cooled fore-optics, and will be commissioned during Summer 2004 in this state before adding the cooled optics (and hence allowing K' band use in Summer 2005). The instrument control hardware and most of the software is a duplicate of that for RATCam.
- **Prototype Spectrograph** - this instrument has been developed in collaboration with John Meaburn of Jodrell Bank. It uses a fibre bundle imaged onto the slit of a nuView spectrograph to give a spectral resolution ~ 4 Å. The fibre bundle is of diameter ~ 10 arcsec, meaning that robotic blind acquisition of a point source onto the target should be possible. A thermoelectrically cooled Apogee camera based around a SITE detector is used to image the spectrum. This instrument is currently undergoing lab testing and will be commissioned in Summer 2004.
- **FRODOSpec** - this instrument[14] is being developed in collaboration with the University of Southampton. It uses a lenslet array to image onto a fibre bundle (again allowing blind acquisition) and custom optics in a dual beam design to provide a resolutions $R \sim 1700 - 6000$. The closed-cycle cooled E2V CCD42-90 detectors are read out using SDSU electronics. This instrument is currently under construction,and is scheduled for commissioning in Autumn 2005.

2.5. Enclosure

The telescope enclosure is a "clam-shell" fully opening design[15] (Figure 1). This has a number of potential advantages. Firstly, no delays are imposed on the observing programme by waiting for dome rotation.[16] Secondly the telescope reaches thermal equilibrium with the outside environment much more quickly, minimizing the effect of dome seeing. We find that thermal equilibrium is established from a large initial $10°$ difference within 30 minutes. A potential disadvantage to a fully open enclosure is susceptibility to windshake. This is further discussed in Sections 2.3.2 above and 3.1 below.

Figure 1. The Liverpool Telescope enclosure (half open).

Table 2. Servo Performance

Tracking Rate (arc sec/s)	Azimuth Error (RMS arc sec)	Altitude Error (RMS arc sec)	Cassegrain Error (RMS arc sec)
15	0.04	0.04	0.12
500	0.16	0.07	3.40

3. PERFORMANCE

First light on the telescope was achieved in July 2003. Since then a programme of commissioning in parallel with scientific operations (Section 4) has been under way in order to progressively improve the telescope performance.

Rather than discuss each of these, we will concentrate in this section on discussing the servo performance of the axes and telescope focus mechanisms as these are the key underlying issues which will determine the eventual overall performance.

3.1. Axis Performance

The top-level astronomical performance specifications presented in Section 2 allowed the derivation servo performance requirements via system error budgets. These are 0.1 arcsec rms for altitude and azimuth axes and 16 arcsec rms for the Cassegrain. Our initial tuning of the azimuth, altitude and Cassegrain rotator axes of the Liverpool Telescope has resulted in the performance recorded in Table 2. Although slightly degraded from factory test results, the servo system is demonstrated to be performing largely within specification.

Of critical importance is the degradation of servo performance with incident wind speed. Modelling[17] shows the generation of H(infinity) controllers in use on the telescope's azimuth and altitude axes are able to perform to specification in winds up to 47 km/hr (13 m/s). Data collection to characterize the performance of wind disturbance rejection is continuing, with early results confirming the predicted performance.

As a test of the resistance of the telescope to windshake, we plot in Figure 2 the image quality measured on 30 second monitoring frames of the QSO's 3C273 and 3C279 in the period February to April 2004 versus the wind speed measured at the telescope site. Comparison with the DIMM data obtained on the same dates shows that the apparent degradation of image quality above 6 m/s is actually a reflection of degradation of the site seeing in such conditions rather than windshake of the telescope structure, and that such performance is maintained up to at least 10 m/s. No data has yet been obtained in wind speeds > 10 m/s.

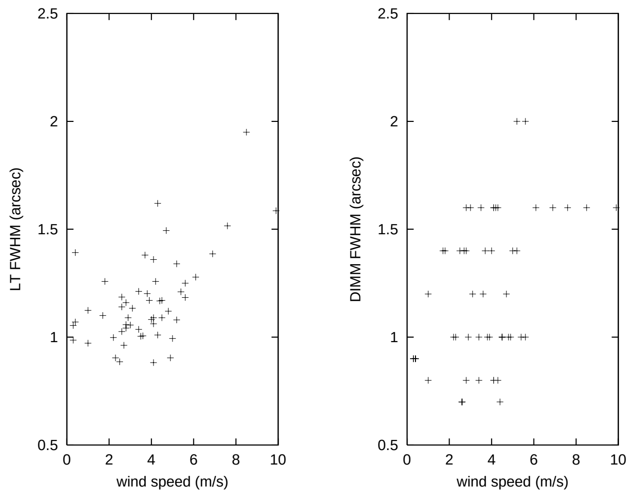

Figure 2. Effect of wind speed on achieved image quality. The left hand plot shows the full width half maximum achieved with the LT versus wind speed. The right hand plot shows similar data obtained with the general site DIMM seeing monitor. Comparison shows that the image quality is dominated by atmospheric turbulence (i.e. not telescope windshake) up to 10 m/s.

We note here that telescope pointing results are currently dominated by non-linearity errors in the incremental encoder system that have not yet been characterized and corrected. As a result, the current pointing model results in an RMS pointing performance of $\sim$ 7 arcsec rms.

3.2. Optical Performance

The telescope optics have been aligned and tested using defocussed star images. Although wavefront sensing evaluation of the optical quality and fine alignment of this system has yet been carried out stellar images have been recorded with a FWHM of 0.7 arc seconds during the commissioning, indicating that the telescope optics, their support and alignment do not significantly affect optical image quality.

The derived focus tolerance at the focal plane of the telescope is $\sim 50\mu$m. At the secondary focus assembly, this translates to an axial position accuracy $\sim 10\mu$m. In order to achieve this positional accuracy, the secondary focus position is servoed to compensate for both telescope orientation and Serrurier truss temperature.

The dependence of focus on temperature due to the expansion of the telescope truss has been measured over the period January – April 2004 and is shown in Figure 3. The expansion coefficient derived (64 μm per °C) is fully consistent with that predicted from the thermal analysis of the structure(60 μm per °C) that was carried out during design. An additional focus effect is the dependence of focus on telescope elevation, due mainly to the compression of the truss by the weight of the structures it supports. This follows a cosine law as predicted by theory, and our measurement of it is shown in Figure 4.

Finally we note that by automatically combining the predictions of the temperature and elevation dependent focus corrections we are able to predict focus at sufficient accuracy from night to night that no calibration of focus at the start of each night has proved necessary. Rather focus frames are just taken occasionally ($\sim$ once per week) in order to act as a quality control and monitor for any long term variations that may appear as the system ages.

4. SCIENCE PROGRAMME

The scientific strengths of the robotic telescope[18] are essentially centred around variability, be that of position, brightness, spectral energy distribution (SED) or any other observable parameter. We describe here some

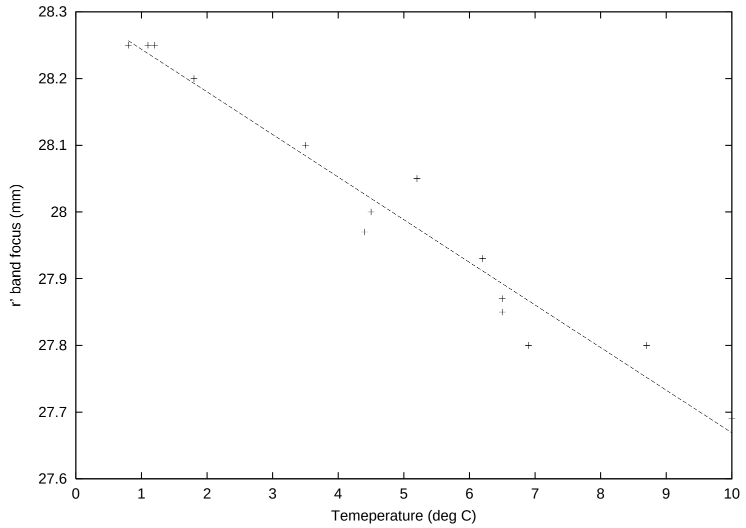

Figure 3. Temperature focus dependence. The fit corresponds to focus $= 28.308 - 0.064\mathrm{T}_{\mathrm{truss}}$.

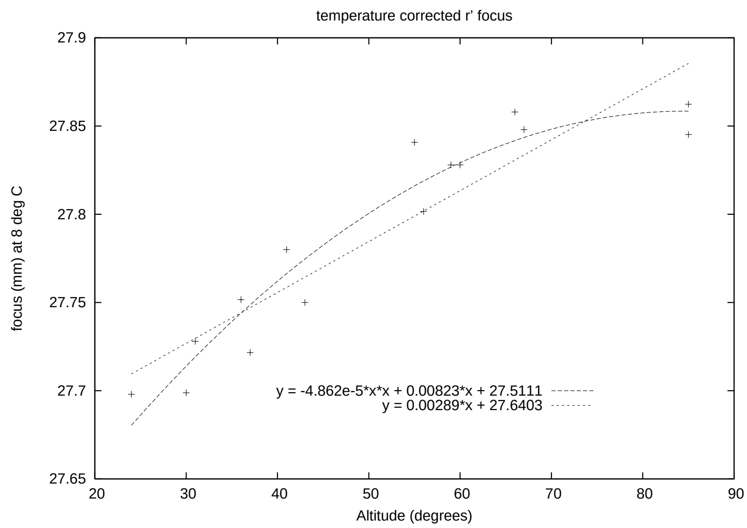

Figure 4. Altitude focus dependence. The final functional form adopted is a cosine function of zenith distance.

Table 3. Sample of LT Science Programmes under way

Multicolour photometric monitoring of CVs
Pixel micro-lensing of stars in M31
A survey for classical novae in M81
Monitoring classical novae light curves in nearby spiral galaxies. Flickering in symbiotic stars
Type Ic supernova light-curves
Triggering of space-based followup for core-collapse supernovae
Contemporaneous monitoring of blazars in co-ordination with space-based X-ray observations
Contemporaneous monitoring of Seyfert galaxies in co-ordination with space-based X-ray observations
GRB prompt optical emission and the first few minutes of optical afterglow

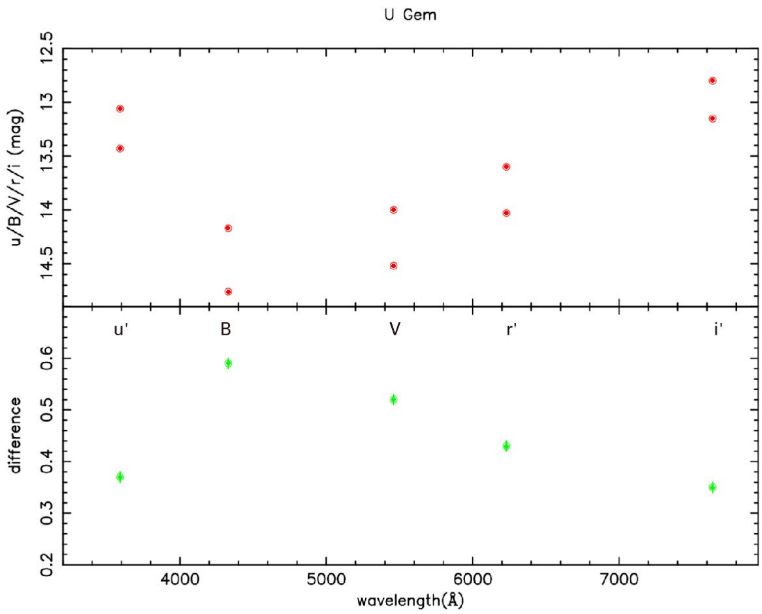

Figure 5. U Geminorum is a well known dwarf nova. Shown in the upper panel of Figure are two epochs (2004-01-20 & 2004-01-21) of LT / RATCam imaging data in $u'BVr'i'$-bands. The various filters are dominated by different emission regions. Very crudely for the five bands, these are the accreting star, inner disc, outer disc, donor star and surrounding cool disc respectively. The lower panel shows the change in each band over the 24 hours between the observations.

programmes already under way which illustrate many of these advantages. The majority of the observations shown here were taken for allocation committee approved programmes and we thank the respective PIs for permission to use the proprietary data in this manner.

Table 3 lists a representative sample of the projects being executed on the LT and shows the range of science targets observed. A few highlights of the science programme so far include:

- D. Steeghs of CfA, Harvard, is obtaining multicolour ($u'BVr'i'$) photometry of a sample of dwarf novae. Long term variable star monitoring has traditionally been in the province of amateur observers and though these data are often of excellent quality, they have mostly been in the visible band. Since different parts of the dwarf nova's SED come from physically distinct parts of the binary system, the variability in each filter contains information about physical processes in the interacting system. Figure 5 shows just two of the epochs taken for this programme.Between the two observations, the star has faded in all bands, but mostly in the visible blue region of the spectrum, showing that the variation is probably occurring predominantly in the accretion disc.

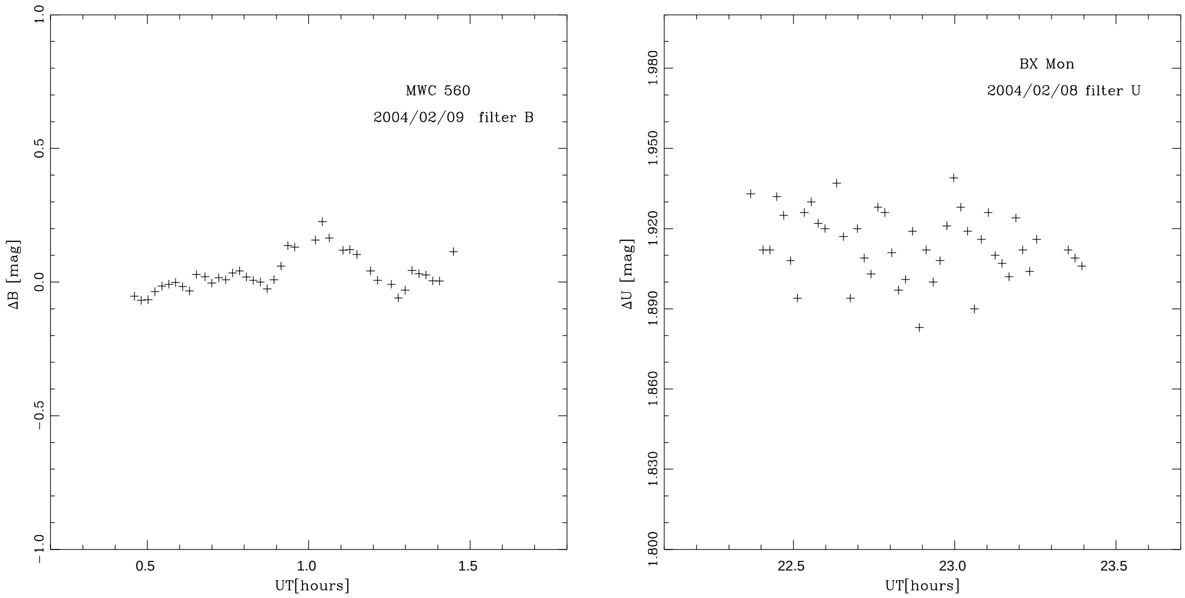

Figure 6. MWC 560 and BX Mon are two symbiotic stars observed during LT / RATCam commissioning as part of a search for rapid variability. Though MWC 560 is clearly variable, no flickering above the level of ± 0.02 mag has been detected in BX Mon.

- R. Zamorov & M.F. Bode have observed symbiotic stars in an endeavor to determine what fraction of the population exhibit the high frequency (period $\sim$ minutes) flickering seen in a subset of cases, if the flickering can be associated with disc instabilities and to search for periodicities which might reveal the spin period of the underlying white dwarf. Figure 6 gives two examples from the LT; one showing clear variability over the period of one hour and the other completely stable with the photometric errors of ± 0.02mag.
- Solar system targets have no fixed celestial coordinates, but assuming the orbit is well known, can be located by the robotic control system at any time without having to resort to pre-calculated lookup tables. Figure 7 shows an image of Comet 2002 T7 LINEAR taken 2004-01-20. In this 100 second exposure, the coma is measured to have radius 32 arcsec, translating to 4.3×10^4km. The programme will continue to monitor a sample of 'normal' comets throughout their orbit to investigate the development of the coma as a function of distance from the Sun.
- Finally, among the very first science observations with the LT was the fortuitously timed SN2004C in NGC3683 (Fig. 7) which occurred only a week preceding the start of LT operations. By triggering a Target of Opportunity programme, Meikle and Mattila[20] were able to measure photometry; $g' = 18.31$, $r' = 16.74$, $i' = 16.37$, $z' = 16.12$ (uncertainties all ± 0.05 mag). Comparison of the $g' - r'$, $r' - i'$ colours with the intrinsic $g - r$, $r - i$ values for a type Ic supernova[19] at 3 weeks past maximum light indicates an extinction exceeding $A_V = 1.0$. Since so few Ic supernovae have well defined light curves, this object is still being routinely monitored by the LT.

4.1. Data rates

The quantity of data distributed to users has increased from 1.5 GBytes in January 2004, the first month of science observations, to 7.5 GBytes in April 2004, the month during which part time robotic operations commenced. The ratio of targeted science data to photometric standard data is 4.3:1. This should decrease very slightly over the Summer months with the increase in photometric conditions. These standards are available equally to all users, so there is no need for PIs to include their required standards in their time allocation. Five per

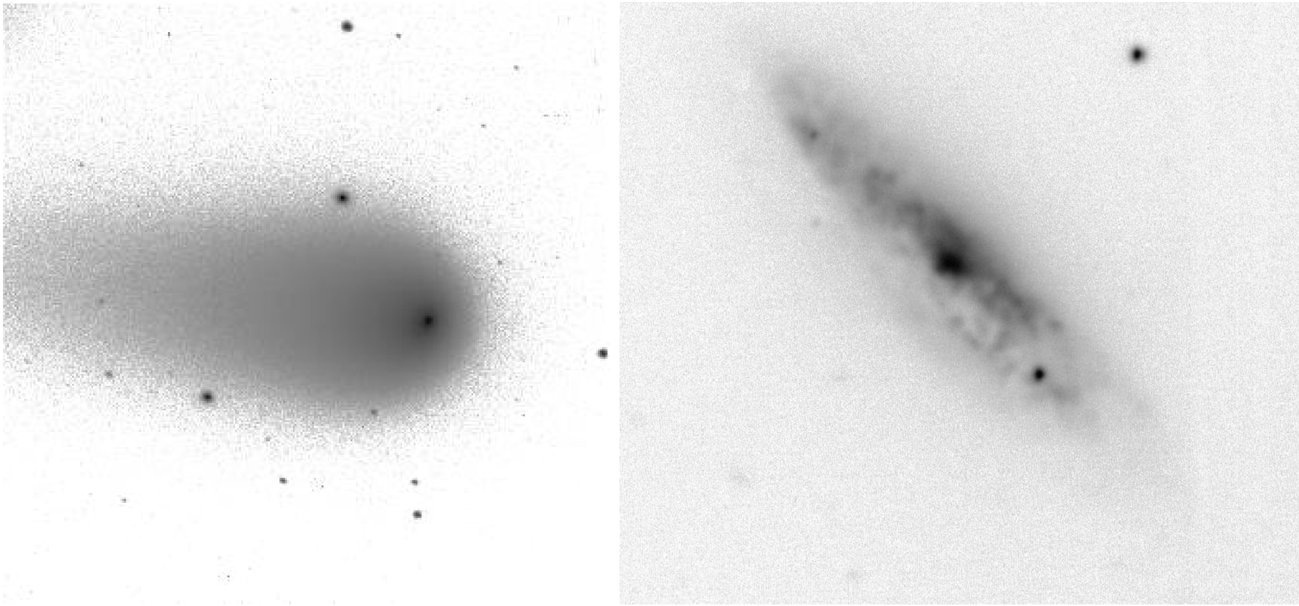

Figure 7. Left panel: Comet C2002T7 LINEAR as observed on 2004-01-20. This was the first test of non-sidereal tracking on the LT. Note the comet nuclear appears more circular than the background stars. **Right panel:** SN2004C observed with LT on 2004-01-16. The SN is the point-like source to the lower right of the galaxy nucleus.

cent of the telescope time has been set aside for educational and public understanding of science use. In the early commissioning phase a greater fraction of the time (15%) has been used in this way (since large bright objects simply make more attractive targets for pointing and configuration tests!). In fact little conclusion should really be drawn from such short term figures, especially given external influences such as the weather, but the increase is as expected and reflects our increasing familiarity with the instrumentation and introduction of more programmes into the schedule. During full time robotic operations, the data rate is expected to be $\sim$ few GBytes per night.

5. CONCLUSIONS

We have presented a description of the Liverpool Telescope and its current performance. Commissioning is ongoing, and we are making good progress to meeting our performance goals. During design we carefully considered the implications of unattended operation for all systems and drove our specifications of the telescope and instrument by appropriate use cases. We have proven that it it possible to build a large, professional class, robotic telescope that is doing science that would be impossible to carry out on a conventionally operated telescope.

ACKNOWLEDGMENTS

We gladly acknowledge the support of the European Union, the UK Particle Physics and Astronomy Research Council and Liverpool John Moores University in providing funds for the construction and continuing operation of the Liverpool Telescope. We thank the staff of the IAC, especially Juan Carlos Perez, for their help and support at the observatory site. We also thank John Meaburn (Jodrell Bank), Peter Meikle (Imperial College), Sue Worswick (Observatory Optics) and Luisa Morales and Phil Charles (Southampton University) for their help in the Liverpool Telescope instrument programme. Finally we thank all the other engineers, astronomers and support staff, both in the UK and on La Palma, who have helped make the Liverpool Telescope project a success.

REFERENCES

1. I.A.Steele, "The Liverpool Telescope", Astronomicsche Nachrichten, **322**, 307-310, 2001
2. I.A. Steele, A.M. Newsam, C.J. Mottram, P. McNerney, "Enabling schools and public access to the Liverpool Robotic Telescope", in *Advanced Global Communications Technologies for Astronomy*, R. I. Kibrick ed., Proc SPIE, **4011**, 133-144, 2000.
3. A. G. Mansfield, "Concept and design of the 2.0-m NGAT: the new generation of astronomical telescopes" in *Advanced Technology Optical/IR Telescopes VI*, Proc SPIE, **3352**, ed. L.M. Stepp, 112-119, 1998
4. A. G. Mansfield, I. P. Baker, "Active approach to telescope design for the new generation of 2.0-m-class telescopes", in *Telescope Structures, Enclosures, Controls, Assembly/Integration/Validation, and Commissioning*, Proc. SPIE, **4004**, eds. T.A.Sebring, T.Andersen, 592-599, 2000
5. M.K. Bowman, M.J.Ford, R.D.J. Lett, D.J. McKay, D. Mucke-Herzberg, M.A. Norbury, "Computing design principles for robotic telescopes", in *Advanced Telescope and Instrumentation Control Software II*, , Proc SPIE, **4848**, ed. H. Lewis, 137-147, 2002.
6. S.N.Fraser, Steele I.A., "Object oriented design of the Liverpool Telescope Robotic Control System", in *Advanced Telescope and Instrumentation Control Software II.* ed. H Lewis, Proc SPIE, **4848**, 443-454, 2002
7. I.A.Steele, "An object model of the Liverpool Telescope", in *Telescope Control Systems III*, Proc SPIE, **3551**, H. Lewis ed., 232-243, 1998.
8. I.A.Steele, D. Carter, "Control Software and Scheduling of the Liverpool Robotic Telescope" in *Telescope Control Systems II*, Proc. SPIE, **3112**, H. Lewis ed., 222 - 233, 1997.
9. Fraser S.N., Steele I.A., "Scheduling the Liverpool Telescope", in *Optimizing Scientific Return for Astronomy through Information Technologies*, Proc SPIE, **5493**, in press, 2004
10. C.J. Mottram, I.A. Steele, L. Morales-Rueda, "Low cost reliable instrumentation for robotic telescopes", in *Ground Based Instrumentation for Astronomy*, Proc SPIE, **5492**, in press, 2004
11. P.J. Surrey, D. Mueke-Herzberg, "Security of remotely operated robotic telescopes", in *Advanced Global Communications Technologies for Astronomy*, Proc SPIE, **4011**, eds. R.I. Kibrick, A. Wallander, 145-156, 2000
12. P. McNerney, I. A. Steele, "Internet Quality of Service between the UK and La Palma 1998 - 1999", in *Advanced Global Communications Technologies for Astronomy*, Proc SPIE, **4011**, 23-32, 2000.
13. R.J. Smith, I.A. Steele, D. Muecke-Herzberg, "Remote secure observing for the Faulkes Telescopes", in *Advanced Software, Control and Communication Systems for Astronomy*, Proc SPIE, **5496**, in press, 2004
14. L. Morales-Rudea, Carter D., Steele I.A., Charles P.A., Worswick S., "The Liverpool Telescope Spectrograph: FRODOSpec", Astronomicsche Nachrichten, **325**, 215-215, 2004
15. A.G. Mansfield,"Open-air approach to enclosure design" in *Telescope Structures, Enclosures, Controls, Assembly/Integration/Validation, and Commissioning*, Proc. SPIE, **4004**, eds. T.A.Sebring, T.Andersen, 171-181, 2000
16. J. Etherton J, P. C. Rees, I. A. Steele, "Telescope design and efficiency", in *Observatory Operations to Optimize Scientific Return II*, Proc SPIE, **4010**, P. J. Quinn ed., 298-313, 2000
17. G.A. Medrano-Cerda, R.D. Lett, P. Rees, "H-Infinity motion control system for a 2 m telescope" in *Survey and Other Telescope Technologies and Discoveries*, Proc SPIE, **4836**, eds J.A. Tyson, S. Wolff , 88-92, 2002.
18. I.A.Steele, "The Liverpool Telescope", in *The Future of the Isaac Newton Group*, New Astronomy Reviews, **45**, N. Walton ed., 45-47, 2001
19. D. Poznanski, A. Gal-Yam, D. Maoz, A.V. Fillippenko, D.C. Leonard, T. Matheson, "Not Color-Blind: Using Multiband Photometry to Classify Supernovae", *PASP*, **114**, 833, 2002
20. W.P.S. Meikle, S. Mattila, IAUC 8270